

## Comparison of acoustic properties between natural and synthetic $\alpha$ -quartz crystals

著者	櫛引 淳一
journal or publication title	Journal of applied physics
volume	94
number	1
page range	295-300
year	2003
URL	<a href="http://hdl.handle.net/10097/35503">http://hdl.handle.net/10097/35503</a>

doi: 10.1063/1.1576891

# Comparison of acoustic properties between natural and synthetic $\alpha$ -quartz crystals

Jun-ichi Kushibiki,<sup>a)</sup> Masanori Ohtagawa, and Izumi Takanaga  
*Department of Electrical Engineering, Tohoku University, Sendai 980-8579, Japan*

(Received 20 December 2002; accepted 31 March 2003)

Accurate measurements of bulk and leaky surface acoustic wave (LSAW) velocities of natural  $\alpha$ -quartz crystal were carried out using the line-focus-beam and plane-wave ultrasonic material characterization systems and then these measured velocities were compared with the velocities of synthetic  $\alpha$ -quartz crystals. Longitudinal velocities of principal  $X$ -,  $Y$ -, and  $Z$ -cut specimens; shear velocities with  $X$ -axis polarized particle displacements of the  $Y$ - and  $Z$ -cut specimens; and LSAW velocities for these three specimens were precisely measured. We found all the velocities for the bulk waves and the LSAWs of natural quartz to be slightly smaller (within 1.00 m/s) than the velocities of synthetic quartz. Therefore, the acoustical physical constants of the natural quartz are very similar to those of synthetic quartz we reported recently. © 2003 American Institute of Physics. [DOI: 10.1063/1.1576891]

## I. INTRODUCTION

Alpha quartz is a widely employed piezoelectric material used for making various electronic devices such as bulk acoustic wave (BAW) and surface acoustic wave (SAW) devices because of its vibration modes with linear temperature coefficients zero and its great physical and chemical stability. The two types of quartz crystals are natural and synthetic. For natural crystals, it was difficult to obtain a large scale of transparent, high-quality quartz crystal ingots useful for devices, due to excessive twins, inclusions, dislocations, and cracks. Thus, growing synthetic quartz was actively studied and homogeneous synthetic quartz crystals were mass produced by the use of autoclaves.<sup>1</sup>

Due to recent demands for higher-frequency and higher-performance devices, homogeneous, high-quality quartz is required more than ever as a base material. It is also important that the acoustical physical constants (elastic, piezoelectric, and dielectric constants, and density) be determined more accurately, and reflected in the quality control and device design. Although the constants have been measured,<sup>2-5</sup> it is doubtful that the determined constant values were accurate because the distinctions between natural and synthetic quartz were not clear.

However, we have developed the line-focus-beam (LFB) and plane-wave (PW) ultrasonic material characterization system<sup>6,7</sup> for highly precise material evaluation techniques and have studied its applications. By changing the ultrasonic devices used, the system can accurately measure the propagation characteristics, viz., velocity and attenuation, of leaky surface acoustic waves (LSAWs) excited on the water-loaded specimen surface with linearly focused ultrasonic waves, and of bulk waves with plane waves. We have demonstrated its usefulness by applying the system to evaluate various materials and device fabrication processes.<sup>8-14</sup> Recently, we started applying the system to evaluate synthetic  $\alpha$  quartz.

Upon comparing results of the measured longitudinal velocities of three principal  $X$ -,  $Y$ -, and  $Z$ -cut plate specimens with those obtained from the numerical calculations using the constants reported by Mason,<sup>2</sup> Benchmann *et al.*,<sup>3</sup> Koga *et al.*,<sup>4</sup> and James,<sup>5</sup> we detected differences of up to 38 m/s for the longitudinal velocities in the  $Z$  axis.<sup>15</sup> Presently, all the constants have been accurately obtained through proper determination procedures.<sup>16</sup> Although the differences may be due to the differences between natural and synthetic quartz, or the different measurement methods (the resonance method and the pulse method), their origination has not always been evident. To identify the causes, it is essential to investigate the differences in acoustic properties between natural and synthetic quartz.

Therefore, as a fundamental study of acoustic properties of natural, and synthetic quartz, we precisely measure bulk wave velocities and LSAW velocities of natural quartz in this paper by preparing three principal  $X$ -,  $Y$ -, and  $Z$ -cut plate specimens to compare with the measured velocity values of synthetic quartz.

## II. MEASURING METHODS

### A. Bulk wave velocities

Velocities of bulk waves were measured by the complex-mode measurement method<sup>17</sup> using radio-frequency (rf) tone burst signals. The experimental arrangement for the measurements is shown in Fig. 1. For the transducer displayed in Fig. 1, we use a ZnO piezoelectric film transducer for the longitudinal wave measurements, and an  $X$ -cut LiNbO<sub>3</sub> plate transducer for the shear wave measurements. Rf pulse signals are applied to the transducer, and converted into ultrasonic waves that propagate through the buffer rod, the couplant, and the specimen. The ultrasonic waves are transmitted, or reflected at each interface, and then returned to the transducer.

<sup>a)</sup>Electronic mail: kushi@ecei.tohoku.ac.jp

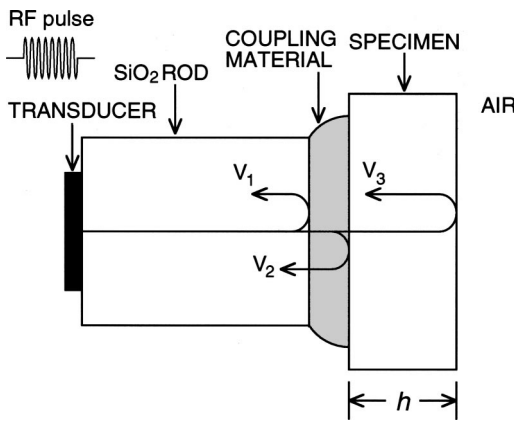


FIG. 1. Experimental arrangement of bulk-velocity measurements of solid specimens using ultrasonic rf pulses.

Pure water is used as the couplant for longitudinal waves, whose layer is an appropriate distance between the ultrasonic device and the specimen, so that the signals reflected from the buffer rod end,  $V_1$ , can be separated from the reflected signals from the front surface of the specimen,  $V_2$ , in the time domain. We measured the phases of the signals reflected from the front surface of the specimen,  $V_2$ , and from the back surface,  $V_3$ . By subtracting the phase of  $V_2$  from the phase of  $V_3$ , the sum of the phase rotations in the specimen ( $-2kh$ ) and at the reflection on the back surface of the specimen ( $\pi$ ) can be obtained as

$$\phi = -2k_\ell h + \pi. \tag{1}$$

Here,  $k_\ell$  is the wave number of longitudinal waves,  $h$  is the thickness of the specimen. A typical example of the frequency response of phase rotation  $\phi$  measured for longitudinal waves of a  $Y$ -cut specimen of natural quartz is shown in Fig. 2 where a thickness of the specimen is  $5034.73 \mu\text{m}$ .  $k_\ell$  is related to the longitudinal velocity in the specimen,  $V_\ell$ , and the angular frequency,  $\omega$ , as  $k_\ell = \omega/V_\ell$ . Therefore, by measuring  $\phi$  and  $h$ , we can determine  $V_\ell$  as follows:

$$V_\ell = -\frac{2\omega h}{\phi - \pi}. \tag{2}$$

For shear-wave measurements, we used phenyl salicylate (salol) as a couplant to bond the buffer rod and the specimen, so the reflected signal from the front surface of the specimen,  $V_2$ , cannot be separated from the reflected signal from the rod end,  $V_1$ , in the time domain. As a result, the phase ro-

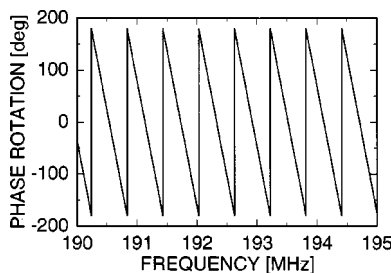


FIG. 2. Typical frequency response of phase rotation measured for longitudinal waves of  $Y$ -cut specimen of natural quartz with a thickness of  $5034.73 \mu\text{m}$  at  $23.01^\circ\text{C}$ .

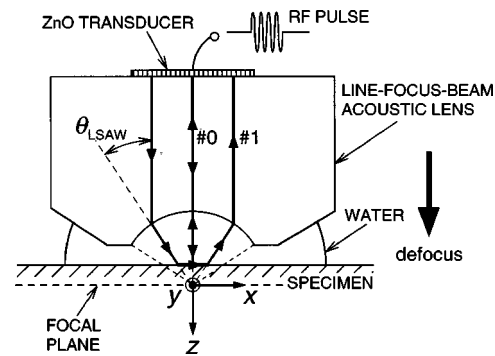


FIG. 3. Cross-sectional geometry of the LFB ultrasonic device describing the principle of  $V(z)$  curve measurements.

tation at the transmission or reflection at the bonding layer,  $\theta_{BL}$ , is contained in the phase rotation,  $\phi$ , to be measured, and we must correct this effect. With the velocity and density values of salol measured in advance as the initial values, we obtained the layer thickness when the measured frequency dependences of the reflection coefficient at the boundaries of the buffer rod, the bonding layer, and the specimen coincide with the calculated frequency dependences based on the ultrasonic transmission line model. Furthermore, the attenuation and velocity of the bonding layer are varied until they coincide with each other. With knowledge of these values,  $\theta_{BL}$  can be calculated and the shear wave velocity of the specimen,  $V_s$ , can be obtained as follows:

$$V_s = -\frac{2\omega h}{\phi - \pi - \theta_{BL}}. \tag{3}$$

In highly precise ultrasonic velocity measurements, it is greatly important to stabilize the measurement temperature environment. Because of this, the ultrasonic device and the specimen are installed in a temperature-controlled chamber that maintains the temperature within  $\pm 0.01^\circ\text{C}$ . The temperature is monitored using a copper-constantan thermocouple calibrated within  $\pm 0.01^\circ\text{C}$  by a standard platinum resistance thermometer.

The thickness of the specimen,  $h$ , is measured using a digital length gauging system with an optical encoder. The measurement accuracy of the thickness is within  $\pm 0.10 \mu\text{m}$ .<sup>18</sup> The thickness is measured only around  $23^\circ\text{C}$ , and during the measurements of the phase rotation, the thickness of each specimen is calculated at each temperature, using the published values of the thermal expansion coefficients.<sup>4</sup>

### B. LSAW velocities

LSAW velocity measurements were conducted using the LFB ultrasonic material characterization (UMC) system.<sup>7</sup> The cross-sectional geometry of the ultrasonic device and the specimen is schematically illustrated in Fig. 3. When the ultrasonic beam is focused on the surface of the specimen ( $z=0$ ), the transducer output is maximized. When the ultrasonic device is moved toward the specimen surface ( $z<0$ ), two components in Fig. 3, viz., directly reflected axial waves (#0) and LSAWs (#1), interfere with each other, and the transducer output is periodically changed so the interference

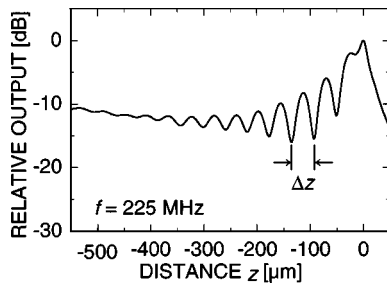


FIG. 4.  $V(z)$  curve measured for Z-axis propagation of Y-cut specimen of natural quartz at 225 MHz.

wave form called a  $V(z)$  curve, as shown in Fig. 4, is obtained. The LSAW velocity,  $V_{LSAW}$ , can be obtained from the oscillation interval  $\Delta z$  of the  $V(z)$  curve using the following equation:

$$V_{LSAW} = \frac{V_W}{\sqrt{1 - \left(1 - \frac{V_W}{2f\Delta z}\right)^2}}, \quad (4)$$

where  $V_W$  is the longitudinal velocity in water and  $f$  is the ultrasonic frequency.

The LFB-UMC system was calibrated using standard specimens<sup>8</sup> of synthetic quartz, of which the acoustical physical constants were determined previously.<sup>16</sup> The relative measurement accuracy of  $V_{LSAW}$  in this system was estimated to be better than  $\pm 0.002\%$  ( $\pm 2\sigma$ ,  $\sigma$  is the standard deviation) at an arbitrary single chosen point on the surface of the specimen and  $\pm 0.003\%$  for a two-dimensional continuous scanning area of  $75 \text{ mm} \times 75 \text{ mm}$ . The absolute accuracy was better than  $\pm 0.005\%$ .

### III. EXPERIMENTS AND RESULTS

#### A. Specimens

Three principal X-, Y-, and Z-cut plate specimens were taken for both natural and synthetic quartz. The specimens of natural quartz were prepared from a high-quality left-handed crystal ingot produced in Brazil, about 5 mm thick, and optically polished on both major faces. The specimens of synthetic quartz were of SAW-grade right-handed crystal ingot (for 3 in. ST-cut wafers) used previously to determine the acoustical physical constants.<sup>16</sup> The parallelism around the center of all the specimens, where velocity measurements were conducted, was within 10 seconds. The influence of the deviation from the parallelism on velocity measurements is negligible.

The inclination of the specimen surface from the crystal-line plane produces errors in velocity measurements. The inclination angles were measured by an x-ray diffractometer and used to correct the velocity values through numerical calculations.

#### B. Bulk wave velocities

Longitudinal velocities of the X-, Y-, and Z-cut specimens, and shear velocities with X-axis polarized particle dis-

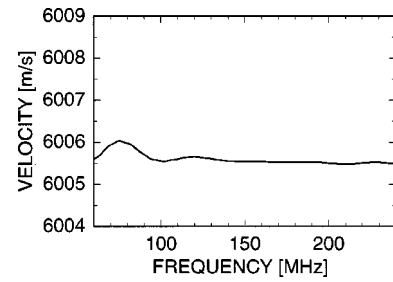


FIG. 5. Measured results of longitudinal velocities of Y-cut specimen of natural quartz.

placements of the Y- and Z-cut specimens were measured at temperatures around 20, 23, and 26 °C. The longitudinal velocities of the Y-cut specimen of natural quartz around 23 °C are shown in Fig. 5 with the velocities plotted as a function of frequency. As observed in Fig. 5, some variations in the measured velocity values exist at frequencies below 150 MHz due to diffraction effects.<sup>17,19,20</sup> Therefore, to reduce the influence of the diffraction effects on the velocity measurements, we chose a frequency range of 165–220 MHz for the longitudinal wave measurements, where the critical frequency in the Fresnel region corresponds to 120 MHz. For the same reason, we chose a frequency range of 115–150 MHz for the shear velocity measurements. The velocities of the specimens are the average velocities in the measured frequency range.

Temperature dependences of the bulk wave velocities of natural and synthetic quartz are shown in Figs. 6 and 7. The measured velocities at each temperature are indicated as circles for natural quartz and as dots for synthetic quartz. The

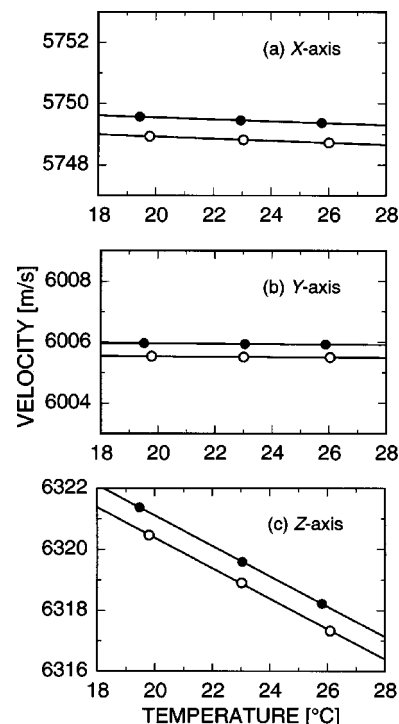


FIG. 6. Temperature dependences of longitudinal velocities of natural and synthetic quartz. Circles represent measured results for natural quartz, and dots represent results for synthetic quartz.

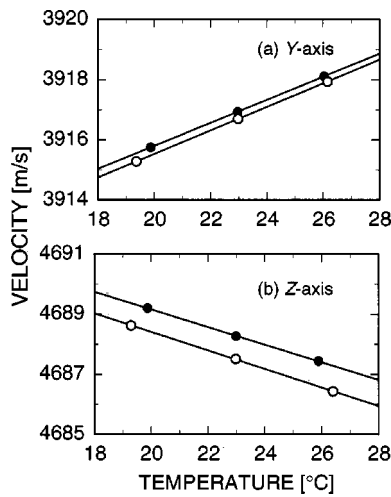


FIG. 7. Temperature dependences of shear velocities of natural and synthetic quartz.

straight lines in Figs. 6 and 7 are the approximated lines fitted by the least-squares method to the measured values. The deviations of measured velocities from the approximated line are very small, 0.03 m/s maximum, for the longitudinal waves of Z-cut specimens of synthetic quartz, and linear temperature dependences were observed from 20 to 26 °C. Therefore, the velocity values at 23.00 °C obtained from the approximated lines were used to compare the acoustic properties between natural and synthetic quartz. The results are given in Table I. The errors in velocity measurements were obtained by considering the variations in the measured phase rotations and the measurement errors in the specimen thicknesses ( $\pm 0.10 \mu\text{m}$ ). Significant differences between natural and synthetic quartz were clearly seen in all cases, smaller (within about 1 m/s) than those of synthetic quartz, even though the velocity differences for the shear waves of Y-cut specimens had values similar to the measurement errors. The differences in temperature coefficients, obtained from the approximated lines, between natural and synthetic quartz are 0.00 (m/s)/°C for longitudinal waves and 0.02 (m/s)/°C maximum in the Z-cut specimens for shear waves, and therefore, the temperature coefficients for each cut surface coincide very well with each other. One cause of the slight differences in shear waves is considered to be the variation in the properties of salol used for the bonding layer in the shear velocity measurements.

TABLE I. Bulk-wave velocities and temperature coefficients of natural and synthetic quartz.

Mode	Plate	Velocity at 23.00 °C (m/s)			Temperature coefficient [(m/s)/°C]		
		Synthetic	Natural	Difference	Synthetic	Natural	Difference
Longitudinal wave	X cut	5749.46 ± 0.25	5748.83 ± 0.20	0.63	-0.03	-0.03	0.00
	Y cut	6005.94 ± 0.20	6005.52 ± 0.17	0.42	-0.01	-0.01	0.00
	Z cut	6319.62 ± 0.30	6318.89 ± 0.22	0.73	-0.50	-0.50	0.00
Shear wave	Y cut	3916.95 ± 0.16	3916.71 ± 0.13	0.24	0.38	0.39	-0.01
	Z cut	4688.28 ± 0.14	4687.49 ± 0.11	0.79	-0.29	-0.31	0.02

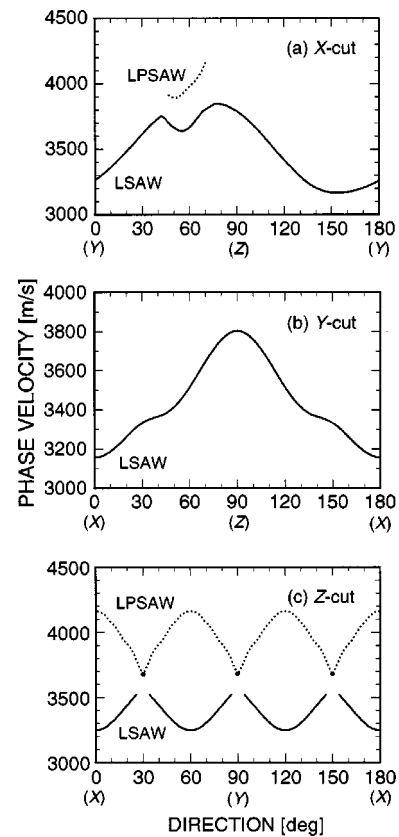


FIG. 8. Angular dependences of LSAW and LPSAW velocities measured for natural quartz around 23 °C.

C. LSAW velocities

LSAW velocities for all of the X-, Y-, and Z-cut specimens were measured at 225 MHz around 23 °C. Figure 8 depicts the typical measured results of angular dependences of LSAW and leaky pseudo-surface wave (LPSAW) (Ref. 6) velocities of natural  $\alpha$  quartz. The propagation characteristics for each specimen exhibit the propagation direction dependence, reflecting the crystal symmetry of  $\alpha$  quartz belonging to class 32 of the trigonal. To compare the velocities between natural and synthetic  $\alpha$ -quartz, we carefully measured the LSAWs velocities for the following selected propagation directions: along the X and Z axes for the Y-cut specimens; along the X and Y axes for the Z-cut specimens; and along the 77° rotated Y axis, with the greatest LSAW velocity, and along the 153° rotated Y axis, with the least LSAW velocity, for the X-cut specimens.



TABLE II. Results of 20 LSAW velocity measurements at around 23 °C.

Plate	Propagation direction	LSAW velocity (m/s)			Temperature (°C)
		Synthetic	Natural	Difference	
X cut	77 °Y axis	3867.47±0.14	3866.46±0.16	1.01	22.85
	153 °Y axis	3181.87±0.21	3181.56±0.21	0.31	22.85
Y cut	X axis	3170.84±0.12	3170.44±0.16	0.40	22.90
	Z axis	3824.04±0.13	3823.22±0.09	0.82	22.91
Z cut	X axis	3266.59±0.10	3266.06±0.10	0.53	22.84
	Y axis	3696.79±0.11	3696.16±0.06	0.63	22.86

The averaged results of 20 LSAW velocity measurements for each specimen are shown in Table II. The measurement errors in velocity are given with the reproducibility of  $\pm 2\sigma$ . Although the temperature stability for each measurement was within  $\pm 0.01$  °C, the averaged temperatures for each set of measurements ranged from 22.81 to 23.01 °C. The temperature variations were due to the measurement environment in the open-space system as shown in Fig. 3 and described in detail in the literature.<sup>6,7</sup> Therefore, using the temperature dependences of LSAW velocities obtained from numerical calculations with the temperature coefficients of the acoustical physical constants of synthetic  $\alpha$  quartz,<sup>16</sup> we corrected the measured LSAW velocities to the values of the measurement temperatures for natural quartz. The corrected amounts were very small, 0.02 m/s maximum. When comparing the velocities, we confirmed that the velocities of natural quartz are smaller (within about 1 m/s) than those of synthetic quartz in the same way as for bulk waves in all cases.

## IV. DISCUSSIONS

### A. Measurements of infrared absorption spectra

Here, the velocity differences between natural and synthetic quartz crystals are investigated in comparison with their infrared absorption spectra. Figure 9 illustrates the results of the infrared absorption spectra for the two Y-cut natural and synthetic  $\alpha$ -quartz plate specimens used for the velocity measurements. These spectra were measured using a Fourier transform infrared (FTIR) spectrometer. The distribution wave form for the natural quartz specimen exhibits many strong peaks corresponding to the impurities contained,<sup>21,22</sup> whereas the synthetic quartz specimen has

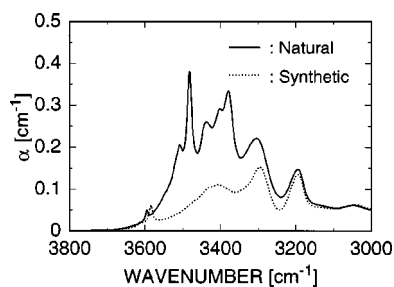


FIG. 9. Infrared absorption spectra of Y-cut specimens of natural and synthetic quartz measured by a FTIR spectrometer.

relatively small absorption with a few peaks. Based on the quality evaluation method, the synthetic quartz crystal was classified as class C using the value of the infrared absorption coefficient,  $\alpha$ , with an  $\alpha$  value of 0.060 at a wave number of  $3585 \text{ cm}^{-1}$ .<sup>23</sup> These spectra for the natural and synthetic quartz specimens are typical waveforms that can be identified in the literature.<sup>21</sup> The velocity differences between the natural and synthetic quartz specimens are considered to be related to the kinds and amounts of the impurities contained.

### B. Comparison with the published values

Our velocities were measured using the rf pulse measurement method according to the experimental and determination procedures we developed previously.<sup>16</sup> The constants of Mason,<sup>2</sup> Bechmann *et al.*,<sup>3</sup> and Koga *et al.*<sup>4</sup> were obtained by the resonance method. For example, there are the following differences between the two methods in determining the constants. First, as a typical example, the Z-axis longitudinal velocity  $V_{Z\ell}$  is related to the elastic constant  $c_{33}^E$  and the density  $\rho$  in the following equation:

$$c_{33}^E = \rho V_{Z\ell}^2. \quad (5)$$

In the pulse method,  $c_{33}^E$  can be obtained by measuring  $V_{Z\ell}$  and  $\rho$ . However, in the resonance method,  $V_{Z\ell}$  cannot be directly measured because no piezoelectricity is involved in Eq. (5). Therefore,  $c_{33}^E$  is obtained using plural equations, and the determined  $c_{33}^E$  may include considerable measurement errors. Second, we paid much attention to specimen preparation, and measured the inclination angles of the crystalline surfaces for the specimens using an x-ray diffractometer. We then corrected the measured velocities within an inclination angle of  $0.01^\circ$  to improve the accuracies of the determined constants. The factors mentioned above are considered to be the main causes for the large differences (over 30 m/s) between our velocity values and those from Mason,<sup>2</sup> and Bechmann *et al.*<sup>3</sup> for the Z-axis longitudinal wave.

## V. CONCLUSIONS

In this article, we accurately measured bulk wave and LSAW velocities of principal X-, Y-, and Z-cut plate specimens prepared from a natural  $\alpha$ -quartz crystal using the LFB/PW ultrasonic material characterization system, and compared the measured velocities with those of synthetic  $\alpha$

quartz we reported recently. As for bulk waves, we measured longitudinal velocities for all the specimens and shear velocities with the *X*-axis polarized particle displacement for the *Y*- and *Z*-cut specimens. LSAW velocities were measured for all the specimens. In all measurements, we found the velocities of natural quartz crystal to be smaller (within about 1 m/s) than those for synthetic quartz crystal. These measured results indicate that there are slight differences in the acoustic properties between natural and synthetic quartz crystals used for electronic devices, but the differences are very small from the acoustical point of view. Large differences (38 m/s maximum for the *Z*-axis longitudinal waves) between the measured velocities and the calculated velocities obtained using the constants of Mason and Bechmann *et al.* are not due to the differences between natural and synthetic quartz crystals, but to some essential errors in the determination methods employed such as the pulse and resonance methods, to differences in the accuracy of the specimen preparation, and/or the confirmation procedure of the specimens for correction.

#### ACKNOWLEDGMENTS

The authors are grateful to M. Arakawa and Y. Ohashi for their technical assistance in the experiments; M. Mochizuki and F. Mishina of Koike Co., Ltd., for supplying the natural quartz crystal; and Y. Okada of Kougakugiken Co., Ltd., for preparing the specimens. This work was supported in part by a Research Grant-in-Aid from the Ministry of Education, Science, and Culture of Japan, and from the Japan Society for the Promotion of Science for the Research for the Future Program.

- <sup>1</sup>J. C. Brice, *Rev. Mod. Phys.* **57**, 105 (1985).
- <sup>2</sup>W. P. Mason, *Piezoelectric Crystals and Their Application to Ultrasonics* (Van Nostrand, New York, 1950), pp. 78–113.
- <sup>3</sup>R. Bechmann, A. D. Ballato, and T. J. Lukaszek, *Proc. IRE* **50**, 1812 (1962).
- <sup>4</sup>I. Koga, M. Aruga, and Y. Yoshinaka, *Phys. Rev.* **109**, 1467 (1958).
- <sup>5</sup>B. J. James, *Proceedings of the 42nd Annual Symposium on Frequency Control* (IEEE, Baltimore, 1988), pp. 146–154.
- <sup>6</sup>J. Kushibiki and N. Chubachi, *IEEE Trans. Sonics Ultrason.* **SU-32**, 189 (1985).
- <sup>7</sup>J. Kushibiki, Y. Ono, Y. Ohashi, and M. Arakawa, *IEEE Trans. Ultrason. Ferroelectr. Freq. Control* **49**, 99 (2002).
- <sup>8</sup>J. Kushibiki and M. Arakawa, *IEEE Trans. Ultrason. Ferroelectr. Freq. Control* **45**, 421 (1998).
- <sup>9</sup>J. Kushibiki, I. Takanaga, M. Arakawa, and T. Sannomiya, *IEEE Trans. Ultrason. Ferroelectr. Freq. Control* **46**, 1315 (1999).
- <sup>10</sup>J. Kushibiki, T. Wei, Y. Ohashi, and A. Tada, *J. Appl. Phys.* **87**, 3113 (2000).
- <sup>11</sup>J. Kushibiki, Y. Ohashi, and Y. Ono, *IEEE Trans. Ultrason. Ferroelectr. Freq. Control* **47**, 1068 (2000).
- <sup>12</sup>J. Kushibiki and M. Miyashita, *J. Appl. Phys.* **89**, 2017 (2001).
- <sup>13</sup>J. Kushibiki, Y. Ohashi, and T. Ujiie, *IEEE Trans. Ultrason. Ferroelectr. Freq. Control* **49**, 454 (2002).
- <sup>14</sup>J. Kushibiki, Y. Ohashi, Y. Ono, and T. Sasamata, *IEEE Trans. Ultrason. Ferroelectr. Freq. Control* **49**, 905 (2002).
- <sup>15</sup>J. Kushibiki, S. Nishiyama, and I. Takanaga, *Electron. Lett.* **36**, 928 (2000).
- <sup>16</sup>J. Kushibiki, I. Takanaga, and S. Nishiyama, *IEEE Trans. Ultrason. Ferroelectr. Freq. Control* **49**, 125 (2002).
- <sup>17</sup>J. Kushibiki and M. Arakawa, *J. Acoust. Soc. Am.* **108**, 564 (2000).
- <sup>18</sup>J. Kushibiki, M. Arakawa, and R. Okabe, *IEEE Trans. Ultrason. Ferroelectr. Freq. Control* **49**, 827 (2002).
- <sup>19</sup>A. O. Williams, Jr., *J. Acoust. Soc. Am.* **23**, 1 (1951).
- <sup>20</sup>E. P. Papadakis, *J. Acoust. Soc. Am.* **40**, 863 (1966).
- <sup>21</sup>A. Kats, *Philips Res. Rep.* **17**, 133 (1962).
- <sup>22</sup>D. M. Dodd and D. B. Fraser, *J. Phys. Chem. Solids* **26**, 673 (1965).
- <sup>23</sup>International Standard IEC No. 60758 (1993).